J|A|C|S
ARTICLES
Published on Web 02/21/2007

Molecular Insights into Azumamide E Histone Deacetylases Inhibitory Activity

Nakia Maulucci,[†] Maria Giovanna Chini,[‡] Simone Di Micco,[‡] Irene Izzo,*[,†] Emiddio Cafaro,[†] Adele Russo,[†] Paola Gallinari,[§] Chantal Paolini,[§] Maria Chiara Nardi,[§] Agostino Casapullo,[‡] Raffaele Riccio,[‡] Giuseppe Bifulco,*[,‡] and Francesco De Riccardis*[,†]

Contribution from the Department of Chemistry, University of Salerno, Via Ponte Don Melillo, 84084 Fisciano, Salerno, Italy, Department of Pharmaceutical Sciences, University of Salerno, Via Ponte Don Melillo, 84084 Fisciano, Salerno, Italy, and Department of Biochemistry, Istituto di Ricerche di Biologia Molecolare "P. Angeletti", Via Pontina, Km 30,600, 00040 Pomezia, Rome, Italy

Received December 7, 2006; E-mail: dericca@unisa.it; bifulco@unisa.it; iizzo@unisa.it

Abstract: Azumamide E, a cyclotetrapeptide isolated from the sponge *Mycale izuensis*, is the most powerful carboxylic acid containing natural histone deacetylase (HDAC) inhibitor known to date. In this paper, we describe design and synthesis of two stereochemical variants of the natural product. These compounds have allowed us to clarify the influence of side chain topology on the HDAC-inhibitory activity. The present contribution also reveals the identity of the recognition pattern between azumamides and the histone deacetylase-like protein (HDLP) model receptor and reports the azumamide E unprecedented isoform selectivity on histone deacetylases class subtypes. From the present studies, a plausible model for the interaction of azumamides with the receptor binding pocket is derived, providing a framework for the rational design of new cyclotetrapeptide-based HDAC inhibitors as antitumor agents.

Introduction

Histone deacetylases (HDACs) are a family of evolutionarily conserved metalloenzymes that, interfering with posttranslational chromatin modification,[1] modulate cell differentiation,[2] apoptosis,[3] cell-cycle progression,[4] and angiogenesis.[5]

For their epigenetic effects on gene expression,[6] HDAC inhibitors have been considered promising anticancer agents and many natural and synthetic inhibitors have entered in clinical trials as possible antitumor agents.[7]

HDAC inhibitors are divided in six distinct groups of zinc chelators.[8] Among them, azumamide A−E (**1**−**5**), recently isolated by Nakao et al. from the marine sponge *Mycale izuensis*, collocate in the small family of hydrophobic cyclotetrapeptides (Figure 1).[9]

Structurally, azumamides include three D-α-amino acids (D-Phe, D-Tyr, D-Ala, D-Val) and a unique β-amino acid assigned as (*Z*,2*S*,3*R*)-3-amino-2-methyl-5-nonenedioic acid 9-amide (amnaa), in azumamides A (**1**), B (**2**), and D (**4**), and (*Z*,2*S*,3*R*)-3-amino-2-methyl-5-nonenedioic acid (amnda), in azumamides C (**3**) and E (**5**). When compared with the other natural cyclopeptide HDAC inhibitors (e.g., trapoxin A (**6**),[10] apicidin D_1,[11] FR-235222,[12] FR-225497,[13] chlamydocin,[14] HC toxin,[15] WF-3161,[16] Cyl-2[17]), azumamides show an intriguing retro-enantio arrangement,[18] displaying an inverse direction of the

[†] Department of Chemistry, University of Salerno.
[‡] Department of Pharmaceutical Sciences, University of Salerno.
[§] Istituto di Ricerche di Biologia Molecolare "P. Angeletti".

(1) Bayle, J. H.; Crabtree, G. R. *Chem. Biol.* **1997**, *4*, 885−888.
(2) Munster, P. N.; Troso-Sandoval, T.; Rosen, N.; Rifkind, R.; Marks, P. A.; Richon, V. M. *Cancer Res.* **2001**, *61*, 8492−8497.
(3) Guo, F.; Sigua, C.; Tao, J.; Bali, P.; Gorge, P.; Li, Y.; Wittmann, S.; Moscinski, L.; Atadja, P.; Bhalla, K. *Cancer Res.* **2004**, *64*, 2580−2589.
(4) (a) Sambucetti, L.; Fischer, D. D.; Zabludoff, S.; Kwon, P. O.; Chamberlin, H.; Trogani, N.; Xu, H.; Cohen, D. *J. Biol. Chem.* **1999**, *274*, 34940−34947. (b) Sato, N.; Ohta, T.; Kitagawa, H.; Kayahara, M.; Ninomiya, I.; Fushida, S.; Fujimura, T.; Nishimura, G.; Shimizu, K.; Miwa, K. *Int. J. Oncol.* **2004**, *24*, 679−685.
(5) Deroanne, C. F.; Bonjean, K.; Servotte, S.; Devy, L.; Colige, A.; Clausse, N.; Blacher, S.; Verdin, E.; Foidart, J.-M.; Nusgens, B. V.; Castronovo, V. *Oncogene* **2002**, *21*, 427−436.
(6) Biel, M.; Wascholowski, V.; Giannis, A. *Angew. Chem.* **2005**, *117*, 3248−3280; *Angew. Chem., Int. Ed.* **2005**, *44*, 3186−3216.
(7) Minucci, S.; Pelicci, P. G. *Nat. Rev. Cancer* **2006**, *6*, 38−51.
(8) Miller, T. A.; Witter, D. J.; Belvedere, S. *J. Med. Chem.* **2003**, *46*, 5097−5116.
(9) (a) Isolation: Nakao, Y.; Yoshida, S.; Matsunaga, S.; Shindoh, N.; Terada, Y.; Nagai, K.; Yamashita, J. K.; Ganesan, A.; van Soest, R. W. M.; Fusetani, N. *Angew. Chem., Int. Ed.* **2006**, *45*, 7553−7557. (b) Synthesis: Izzo, I.; Maulucci, N.; Bifulco, G.; De Riccardis, F. *Angew. Chem., Int. Ed.* **2006**, *45*, 7557−7560.
(10) (a) Itazaki, H.; Nagashima, K.; Sugita, K.; Yoshida, H.; Kawamura, Y.; Yasuda, Y.; Matsumoto, K.; Ishii, K.; Uotani, N.; Nakai, H.; Terui, A.; Yoshimatsu, S.; Ikenishi, Y.; Nakagawa, Y. *J. Antibiot.* **1990**, *43*, 1524−1532. (b) Kijima, M.; Yoshida, M.; Sugita, K.; Horinouchi, S.; Beppu, T. *J. Biol. Chem.* **1993**, *268*, 22429−22435. (c) Taunton, J.; Hassig, C. A.; Schreiber, S. L. *Science* **1996**, *272*, 408−411.
(11) Singh, S. B.; Zink, D. L.; Polishook, J. D.; Dombrowski, A. W.; Darkin-Rattray, S. J.; Schmatz, D. M.; Goetz, M. A. *Tetrahedron Lett.* **1996**, *37*, 8077−8080.
(12) (a) Mori, H.; Urano, Y.; Abe, F.; Furukawa, S.; Tsurumi, Y.; Sakamoto, K.; Hashimoto, M.; Takase, S.; Hino, M.; Fujii, T. *J. Antibiot.* **2003**, *56*, 72−79. (b) Mori, H.; Urano, Y.; Abe, F.; Furukawa, S.; Furukawa, S.; Sakai, F.; Hino, M.; Fujii, T. *J. Antibiot.* **2003**, *56*, 80−86.
(13) Mori, H.; Fumie, A.; Seiji, Y.; Shigehiro, T.; Motohiro, H. PCT Application WO 00/08048, 2000.
(14) Closse, A.; Huguenin, R. *Helv. Chim. Acta* **1974**, *57*, 533−545.
(15) Pringle, R. B. *Plant Physiol.* **1970**, *46*, 45−49.

10.1021/ja0686256 CCC: $37.00

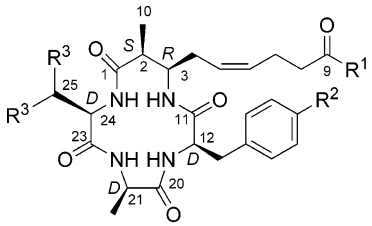

	R^1	R^2	R^3	IC_{50} (μM)[a]
azumamide A (**1**):	NH_2	H	CH_3	0.045
B (**2**):	NH_2	OH	CH_3	0.11
C (**3**):	OH	OH	CH_3	0.11
D (**4**):	NH_2	H	H	1.3
E (**5**):	OH	H	CH_3	0.064

[a]Against the crude enzymes extracted from K562 cells.

Figure 1. Structures of azumamides A−E (**1**−**5**).

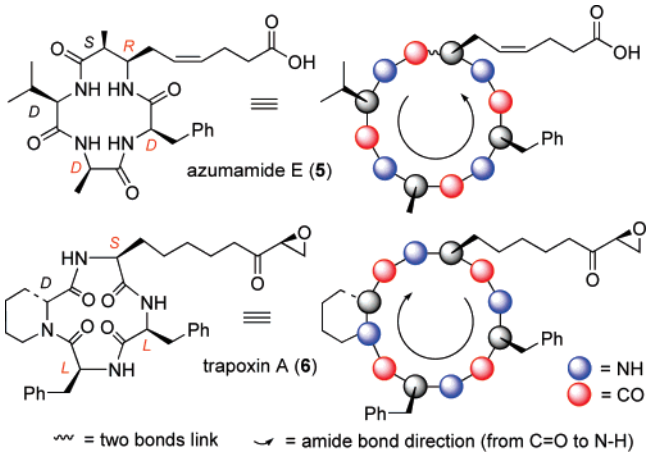

Figure 2. Schematic representation of (+)-azumamide E (**5**) and trapoxin A (**6**).

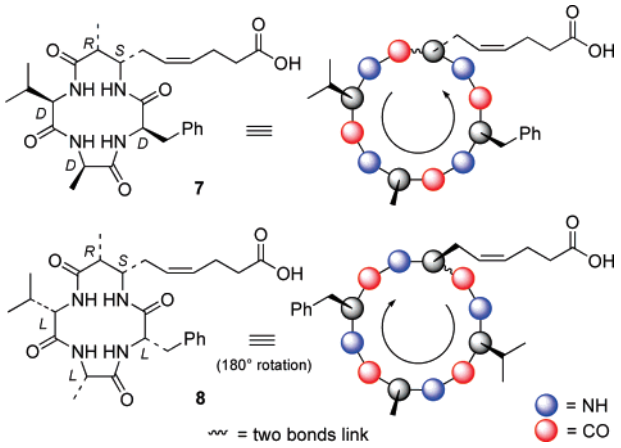

Figure 3. Formulas and schematic representation of the two target (+)-azumamide E (**5**) stereoisomers: (2*R*,3*S*)-azumamide E (**7**) and (−)-azumamide E (**8**).

amide bonds and contemporary opposite absolute configuration at the side chain-bearing stereogenic centers (Figure 2).

Though a zinc-chelating residue is necessary for the HDAC inhibitory activity, there is strong evidence that the tetrapeptide three-dimensional appendage orientation significantly influences the ligand−protein recognition pattern.[19] However, our understanding of the HDAC−ligand interaction is limited to small molecule inhibitors,[20] being published only one contribution analyzing the binding contacts between the histone deacetylase-like protein (HDLP) and the tetracyclopeptide framework.[21]

The scarce information on the role played by the cyclic tetrapeptide cap group in the HDAC recognition process prompted us to explore the molecular details of the interaction between azumamide E (**5**)[22] and the HDLP binding pocket.[20a,23] Subsequently, with the aim to probe the effects of the side chains' relative orientation and the role of the peptide bond direction on the binding efficiency, we synthesized two carefully chosen stereochemical variants of natural (+)-azumamide E (**5**): (2*R*,3*S*)-azumamide E (**7**) and (−)-azumamide E (**8**, Figure 3), carried out the docking study, and verified their HDAC inhibitory activities.

The first selected target, compound **7**, presents a configurationally inverted amnda residue[24] so that the C3-linked esenoic side chain results topologically off-register. The second target, **8**, being the enantiomer of azumamide E, displays complete

(16) Umehara, K.; Nakahara, K.; Kiyoto, S.; Iwami, M.; Okamoto, M.; Tanaka, H.; Kohsaka, M.; Aoki, H.; Imanaka, H. *J. Antibiot.* **1983**, *36*, 478−483.
(17) Hirota, A.; Suzuki, A.; Suzuki, H.; Tamura, S. *Agric. Biol. Chem.* **1973**, *37*, 643−647.
(18) (a) Shemyakin, M. M.; Ovchinnikov, Yu, A.; Ivanov, V. T. *Angew. Chem., Int. Ed.* **1969**, *8*, 492−499. (b) Prelog, V.; Gerlach, H. *Helv. Chim. Acta* **1964**, *47*, 2288−2294. (c) Goodman, M.; Chorev, M. *Acc. Chem. Res.* **1979**, *12*, 1−7.
(19) (a) Colletti, S. L.; Myers, R. W.; Darkin-Rattray, S. J.; Gurnett, A. M.; Dulski, P. M.; Galuska, S.; Allocco, J. J.; Ayer, M. B.; Li, C.; Lim, J.; Crumley, T. M.; Cannova, C.; Schmatz, D. M.; Wyvratt, M. J.; Fisher, M. H.; Meinke, P. T. *Bioorg. Med. Chem. Lett.* **2001**, *11*, 113−117. (b) Furumai, R.; Komatsu, Y.; Nishino, N.; Khochbin, S.; Yoshida, M.; Horinouchi, S. *Proc. Natl. Acad. Sci. U.S.A.* **2001**, *98*, 87−92. (c) Kim, S.-D. *J. Biochem. Mol. Biol.* **1995**, *28*, 227−231. (d) Colletti, S. L.; Myers, R. W.; Darkin-Rattray, S. J.; Gurnett, A. M.; Dulski, P. M.; Galuska, S.; Allocco, J. J.; Ayer, M. B.; Li, C.; Lim, J.; Crumley, T. M.; Cannova, C.; Schmatz, D. M.; Wyvratt, M. J.; Fisher, M. H.; Meinke, P. T. *Bioorg. Med. Chem. Lett.* **2001**, *11*, 107−111.
(20) (a) Finnin, M. S.; Donigian, J. R.; Cohen, A.; Richon, V. M.; Rifkind, R. A.; Marks, P. A.; Breslow, R.; Pavletich, N. P. *Nature* **1999**, *401*, 188−193. (b) Vannini, A.; Volpari, C.; Filocamo, G.; Casavola, E. C.; Brunetti, M.; Renzoni, D.; Chakravarty, P.; Paolini, C.; De Francesco, R.; Gallinari, P.; Steinkühler, C.; Di Marco, S. *Proc. Natl. Acad. Sci. U.S.A.* **2004**, *101*, 15064−15069.
(21) Rodriquez, M.; Terracciano, S.; Cini, E.; Settembrini, G.; Bruno, I.; Bifulco, G.; Taddei, M.; Gomez-Paloma, L. *Angew. Chem., Int. Ed.* **2006**, *45*, 423−427.
(22) The reported biological activities were performed on synthetic azumamide E. The analytical data ($[\alpha]_D$, electrospray mass spectrometry, ^1H and ^{13}C NMR spectrometry) measured on the synthetic sample were virtually indistinguishable from those reported for the natural product.
(23) Since there is no X-ray structure of human HDAC1 available now, we have used the monomer form of the HDLP X-ray structure as receptor model. A sequence alignment shows a 35.2% sequence identity of HDLP and human HDAC1. The residues around the HDLP zinc-binding site are completely conserved in human HDAC1 and all of the hydrophobic residues that make up the 11 Å channel in HDLP are identical in HDAC1. Most of the residues making up the 14 Å internal cavity are either identical or conservatively substituted in HDAC1 and, as can be expected from the high degree of sequence similarity, HDAC has the same structural features of HDLP described above.
(24) Both the *β*-amino acid stereogenic centers were inverted to retain the same relative configuration of the 3-amino-2-methyl-5-nonendioic acid.
(25) (a) Grüenewald, J. Marahiel, M. A. *Microbiol. Mol. Biol. Rev.* **2006**, *70*, 121−146. (b) Hamada, Y.; Shioiri, T. *Chem. Rev.* **2005**, *105*, 4441−4482.
(26) In a recently reported SAR study on cyclic hydroxamic acid containing cyclopeptides (designed as hybrid of trichostatin and trapoxin, see: Komatsu, Y.; Tomizaki, K.-Y.; Tsukamoto, M.; Kato, T.; Nishino, N.; Sato, S.; Yamori, T.; Tsuruo, T.; Furumai, R.; Yoshida, M.; Horinouchi, S.; Hayashi, H. *Cancer Res.* **2001**, *61*, 4459−4466), the HDAC inhibitory potency of different amino acid D/L combinations was directly related to the hydrophobicity of the molecules (higher hydrophobicity meant higher membrane permeability). This assumption contrasted with the weak activity (2 orders of magnitude lower) observed for one of the synthesized derivatives (showing HPLC retention time comparable with those of the cognate compounds). We believe that biological activity should be, more appropriately, attributable to the tetrapeptide−receptor interaction modes. Our studies clarify some aspects of the binding at molecular level.

Scheme 1. Synthesis of Compound **7**[a]

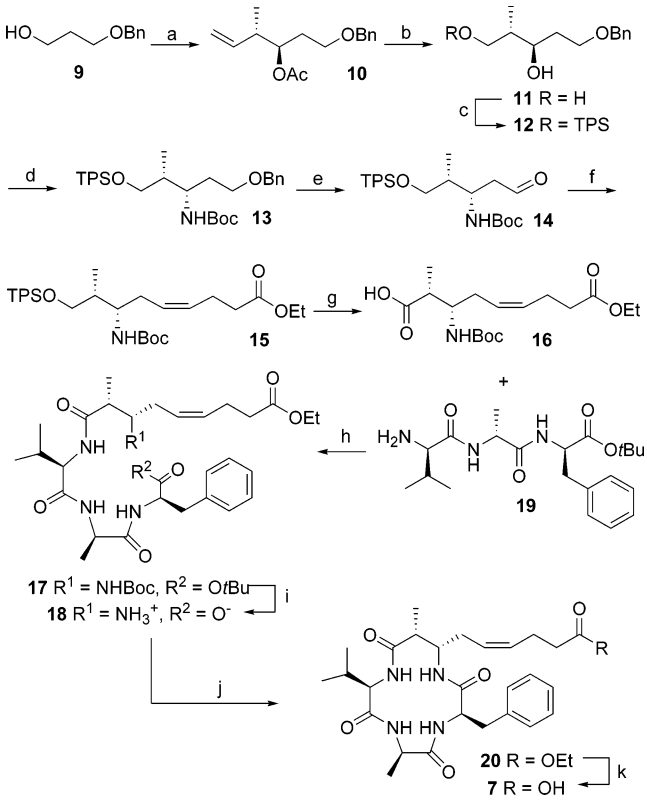

[a] Reagents and conditions: (a) i. oxalyl chloride, DMSO, Et_3N, CH_2Cl_2, −78 °C; ii. (−)-Ipc_2BOMe, (*E*)-2-butene, *t*-BuOK, *n*-BuLi, $BF_3{\cdot}Et_2O$, THF, −78 °C, then aq NaOH, H_2O_2; iii. Ac_2O, Py, CH_2Cl_2, 68%, over three steps; (b) i. O_3, CH_2Cl_2, then PPh_3; ii. $NaBH_4$, EtOH; iii. K_2CO_3, MeOH, 64% over three steps; (c) TPSCl, DMAP, Py, CH_2Cl_2, 93%; (d) i. MsCl, Et_3N, THF; ii. NaN_3, DMF, 60 °C, iii. H_2, Pt_2O, AcOEt; iiii. Boc_2O, Et_3N, CH_2Cl_2, 71% over four steps; (e) i. H_2, Pd/C, EtOH; ii. oxalyl chloride, DMSO, Et_3N, CH_2Cl_2, −78 °C, 80% over two steps. (f) i. $BrPh_3PCH_2CH_2CH_2CO_2Et$, KHMDS, THF, −78 °C to r.t., 94%; (g) i. HF/Py, Py; ii. TEMPO, phospate buffer, $NaClO_2$, NaClO, CH_3CN, 59%, over two steps; (h) EDC, HOBt, DIPEA, CH_2Cl_2, 87%; (i) TFA/CH_2Cl_2 1:1, quant.; (j) FDPP, DIPEA, DMF, 3d, 29%; (k) LiOH, H_2O/THF, 0 °C, 79%.

side chain reversal. However, for the intrinsic stereochemical arrangement of the azumamides, if compound **8** is turned in the plane 180°, it shows a side chain topology comparable to that of natural azumamide E (Val and Phe result in positionally exchanged and configurationally inverted) and a reversed peptide bond orientation (similar to that of trapoxin A (**6**) and the related natural cyclotetrapeptides, see Figure 2).

Cyclopeptides isolated from natural sources represent the latest products of a constant phylogenetic molecular morphology optimization.[25] This means that the effects of stereochemical/framework alterations could, in principle, conspicuously affect biological activity. With the synthesis and docking studies on stereoisomeric azumamide derivatives **7** and **8**, we probe the morphological role of the residue positioning and the impact of the amide bond peptide core orientation on biological activity.[26]

As a consequence of this study, we evidence a rare case in which the enantiomer of a putative peptide ligand, though acting on a chiroselective receptor, retains biological activity.[27]

This contribution reports on the synthesis of (2*R*,3*S*)-azumamide E (**7**) and (−)-azumamide E (**8**). It presents a 3D model for the interaction of **5**, **7**, and **8**, with the HDLP active site, and fully discloses the HDAC inhibitory activities exerted

Scheme 2. Synthesis of Compound **8**[a]

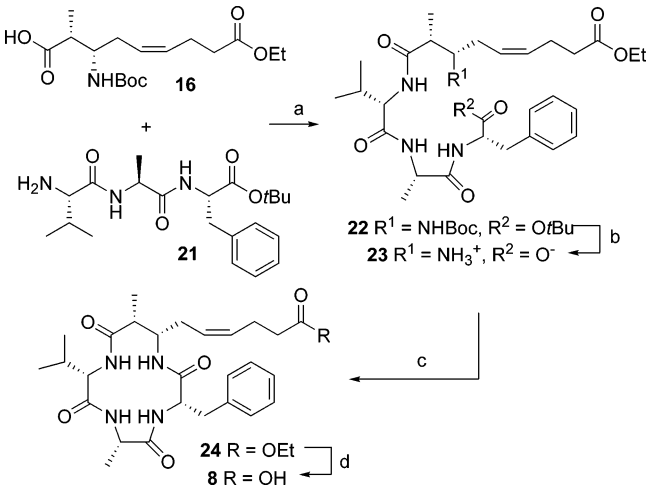

[a] Reagents and conditions: (a) EDC, HOBt, DIPEA, CH_2Cl_2, 72%; (b) TFA/CH_2Cl_2; 1:1, quant.; (c) FDPP, DIPEA, DMF, 3d, 54%; (d) LiOH, H_2O/THF, 0 °C, 75%.

by azumamide E (**5**) against the HeLa cell nuclear extract and against class I (HDACs 1−3 and 8) and class II (HDACs 4−7 and 9) histone deacetylase subtypes[28] and those of **7** and **8** against the HeLa cell nuclear extract.

Results and Discussion

Synthesis of (2*R*,3*S*)-Azumamide E (7) and (−)-Azumamide E (8). The elaboration of (2*R*,3*S*)-azumamide E (**7**, Scheme 1) was accomplished by a route previously reported for the successful (+)-azumamide E (**5**) synthesis.[9b] The "unnatural" (*Z*,2*R*,3*S*)-3-[(*tert*-butyloxycarbonyl)amino]-2-methyl-5-nonenedioic acid, 9-ethyl ester (**16**, Scheme 1) residue, whose synthesis started from commercially available 3-benzyloxy propanol and relied on the Brown's crotylboration reaction,[29] was joined to the linear all-D tripeptide **19**, synthesized following the classic solution-phase protocol.[9b]

Contemporary terminal carboxy and amino group deprotection, followed by an FDPP-mediated macroclactamization reaction,[30] furnished the (*Z*,2*R*,3*S*)-azumamide E ethyl ester (**20**), which liberated target compound **7** upon hydrolysis in the presence of LiOH (2.7% overall yield, starting from **9**).

The synthesis of **8** proceeded uneventfully and followed the same strategy reported for its enantiomer **5** (Scheme 2).[9b] This time, the bis-protected β-amino acid **16** was linked to the linear

(27) The term "chiroselective" is used in opposition to "nonspecific". Typical nonspecific biological actions are exerted on membranes. For the action of enantiomers of bioactive compounds on nonspecific target, see, for example: Juvvadi, P.; Vunnam, S.; Merrifield, R. B. *J. Am. Chem. Soc.* **1996**, *118*, 8989−8997. Vunnam, S.; Juvvadi, P.; Rotondi, K. S.; Merrifield, R. B. *J. Pept. Res.* **1998**, *51*, 38−44. Shemyakin, M. M.; Ovchinnikov, Y. A.; Ivanov, V. T.; Evstratov, A. V. *Nature* **1967**, *213*, 412−413. Shemyakin, M. M.; Ovchinnikov, Y. A.; Ivanov, V. T. *Angew. Chem., Int. Ed.* **1969**, *8*, 492−499. For the action of enantiomers of bioactive compounds on chiroselective target, see, for example: Bednarek, M. A.; Silva, M. V.; Arison, B.; MacNeil, T.; Kalyani, R. N.; Huang, R.-R. C.; Weinberg, D. H. *Peptides* **1999**, *20*, 401−409 (in which is described a significant drop of potency of the enantio-analog of the cyclic peptide MT-II). Guichard, G.; Benkirane, N.; Zeder-Lutz, G.; Van Regenmortel, M. H. V.; Briand, J.-P.; Muller, S. *Proc. Natl. Acad. Sci. U.S.A.* **1994**, *91*, 9765−9769 (in which is described the immunoglobulin IgG3 response on an enantiomeric form of an immunogenic peptide. Interestingly, no cross-response was observed for IgG1, IgG2a, and IgG2b antibodies).

(28) Johnstone, R. W. *Nat. Rev. Drug Discovery* **2002**, *1*, 287−299.

(29) Brown, H. C.; Bhat, K. S. *J. Am. Chem. Soc.* **1986**, *108*, 293−294.

(30) (a) Chen, S.; Xu, J. *Tetrahedron Lett.* **1991**, *32*, 6711−6714. (b) Dudash, J., Jr.; Jiang, J.; Mayer, S. C.; Joullie, M. M. *Synth. Commun.* **1993**, *23*, 349−356.

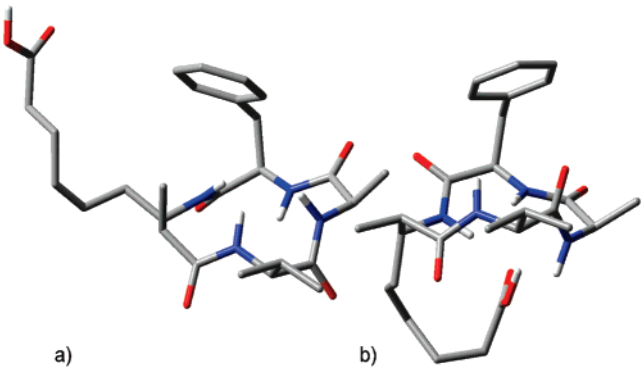

Figure 4. NMR solution-state conformations of **5** and **7** obtained by restrained MD calculations, using ROESY (t_{mix}=100 ms, 300 K) data collected at 600 MHz in [D_6]DMSO (see Supporting Information).

all-L tripeptide **21**. After that, (−)-azumamide E (**8**) was formed in two steps and 4.0% overall yield (starting from **9**).

NMR and Docking Studies. Docking studies were performed on (+)-azumamide E (**5**), (2*R*,3*S*)-azumamide E (**7**), and (−)-azumamide E (**8**), with the HDLP[20a,31] binding pocket, using AutoDock 3.0.5 software,[32] which has been successfully used in the interpretation of the inhibitory activity of several HDAC ligands.[33] The DMSO solution-state structures were obtained by 2D-NMR spectroscopy (Figure 4 a, b) and were used as the initial conformations in the docking study. The NMR structure backbone analysis of **7** (Figure 4b), in analogy with that reported for **5** (Figure 4a),[9b] did not reveal the presence of any identifiable turns or defined secondary structure. On the other side, it showed a marked difference in the peptide bond spatial arrangement and an unexpected hydrogen bond between the C9 carboxy group and the NH of the D-Ala residue.

The partial charges of the three ligands (**5**, **7**, and **8**), of the zinc ion, and of the amino acids involved in the catalytic center (A169, H170, D168, D258) have been calculated at DFT B3LYP level and 6-31G(d) basis set using the ChelpG[34] method for population analysis and have been used in the subsequent docking calculations.

In the theoretical studies, we have considered the amnda residue carboxy group functionality as dissociated at physiological pH and, consequently, deprotonated in the calculations. The carboxylate moiety is of primary importance for its interactions network: it coordinates the zinc ion and establishes hydrogen bonds with $H^{\epsilon 2}$ of H131 and H132, and OH of Y297 (not shown).[35] Moreover, the C3 linked esenoic chain makes stabilizing hydrophobic contacts with the zinc-containing tubular pocket. The macrolactam portion is accommodated in a shallow groove, establishing van der Waals interactions and hydrogen bonds with the receptor counterpart, formed by H170, Y196, A197, F198, and F200 residues (Figure 5).

The tetrapeptide core extends its hydrophobic contacts thanks to the D-Phe side chain, which is accommodated in a deep pocket

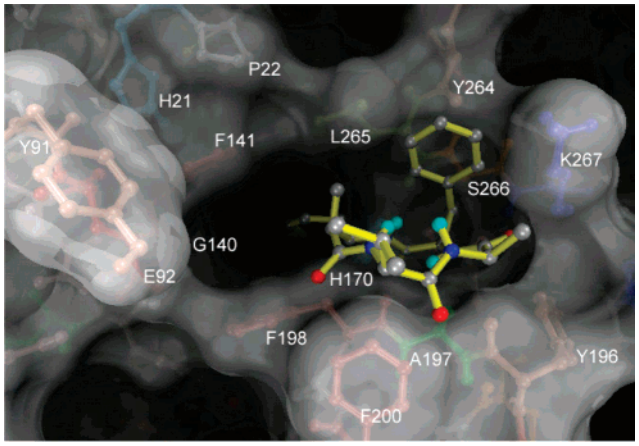

Figure 5. 3D model of the interaction between azumamide E (**5**) and the HDLP binding site. The protein is represented by molecular surface and sticks and balls. **5** is depicted by sticks (yellow) and balls (by atom type: C, gray; polar H, sky blue; N, dark blue; O, red). The figure highlights essential interactions: the phenyl group is located in a hydrophobic pocket and the tetrapeptide core interacts with a shallow cavity on the receptor surface. The amnda side chain establishes interactions with the 11 Å hydrophobic channel and with the zinc ion contained at the bottom.

delimited by the Y264, L265, S266, and K267 residues, enveloping the phenyl ring. The D-Val side chain points outside the receptor.

The (2*R*,3*S*)-azumamide E (**7**) is characterized by a configurationally inverted amnda residue and topologically repositioned D-Phe and D-Val side chains. In contrast with a single and defined family of conformations representing the efficient binding mode for natural azumamide E (**5**), this time we obtained three different conformation families, accounting for three independent, low affinity, binding modes (Figure 6 a−c).

In the first conformation (Figure 6a), which has the best binding energy among the three, the macrolactam ring interacts with a shallow pocket delimited by E92, H170, F141, F198, G140, L265, and H132.[35] The D-Val side chain enjoys van der Waals interactions with H170, F198, and L265. The D-Phe side chain establishes stabilizing hydrophobic interactions with F198 and F200 residues. Although the above-reported hydrophobic interactions are maintained, the spatial positioning of the amnda chain prevents, in this arrangement, an efficient coordination of the carboxylate group to the zinc ion, as witnessed by the distance of about 7 Å between the two groups, suggesting lack in the binding activity.

In the second conformation, **7** coordinates the zinc ion, but the interactions expected for the phenyl and the isopropyl groups are lost (Figure 6b). In the third model (Figure 6c), the phenyl group is placed in the same hydrophobic cavity found for **5**, but a minor number of interactions are observed; moreover, only one of the two oxygens of the carboxylate function coordinates the zinc ion.

In (−)-azumamide E (**8**), the complete configuration inversion maintains the three-dimensional side chains' relative positioning. Our docking studies indicate that the amnda chain and the tetrapeptide core of the two docked enantiomers (**8** and **5**) fill equivalent spaces, and the valine and phenylalanine residues inverted positions give minor perturbations (Figure 7). Moreover, the amnda side chain exerts the same set of interactions observed in **5**, with the tubular hydrophobic pocket and the zinc-

(31) Wang, D-F.; Wiest, O.; Helquist, P.; Lan-Hargest, H-Y.; Wiech, N. L. *J. Med. Chem.* **2004**, *47*, 3409−3417.
(32) Morris, G. M.; Goodsell, D. S.; Halliday, R. S.; Huey, R.; Hart, W. E.; Belew, R. K.; Olson, A. J. *J. Comp. Chem.* **1998**, *19*, 1639−1662.
(33) (a) Wang, D-F.; Helquist, P.; Wiech, N. L.; Wiest, O. *J. Med. Chem.* **2005**, *48*, 6936−6947. (b) Park, H.; Lee, S. *J. Comput.-Aided Mol. Des.* **2004**, *18*, 375−388.
(34) Breneman, C. M.; Wiberg, K. B. *J. Comp. Chem.* **1990**, *11*, 361−373.
(35) H131, H132, and Y297 are not shown in Figures 5−7 because they are too deep in the channel. They are reported (in the 3D models of the interaction between **5** and **8** with the HDLP binding site) in Figure S3 and S4 of the Supporting Information.

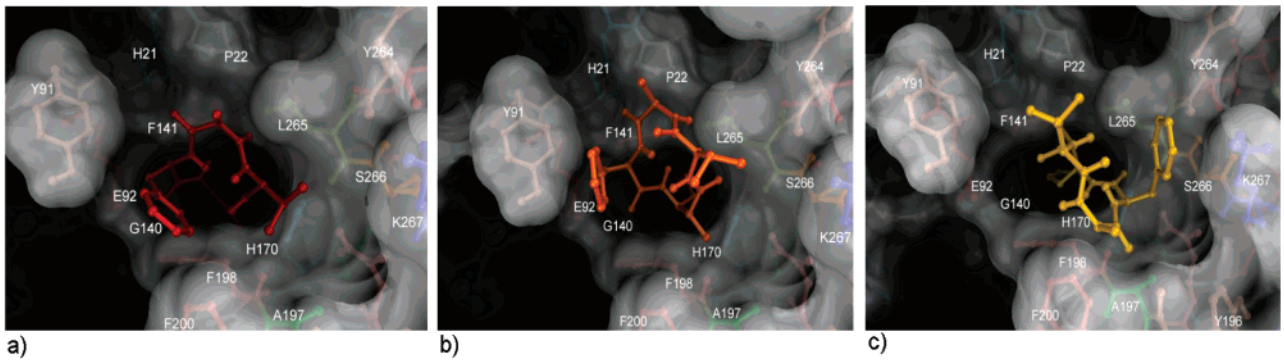

Figure 6. 3D model of the interaction between **7** and the HDLP binding site. The protein is represented by molecular surface and sticks and balls. **7** is shown in three different docking poses (by sticks and balls): (a) in red is the best binding energy conformation but it does not coordinate the Zn; (b) in orange is the best binding energy conformation that coordinates zinc ion; (c) in yellow is the best docking energy conformation.

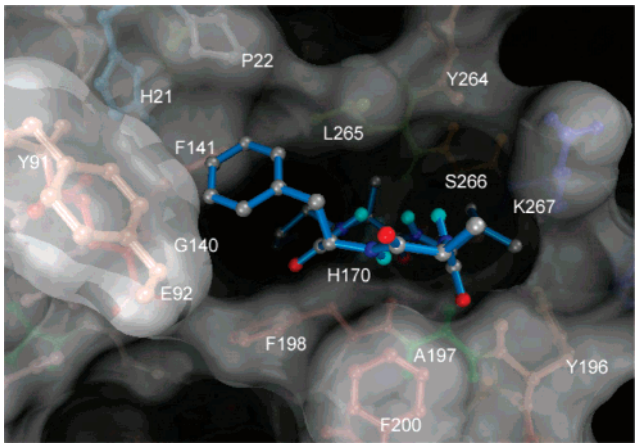

Figure 7. 3D model of the interaction between **8** and the HDLP binding site. The protein is represented by molecular surface and sticks and balls. **8** is depicted by sticks (blue) and balls (by atom type: C, gray; polar H, sky blue; N, dark blue; O, red). The figure highlights essential interactions: the phenyl establishes hydrophobic interactions and the tetrapeptide core interacts with a shallow cavity on the receptor surface The amnda side chain establishes interactions with the 11 Å hydrophobic channel and with the zinc ion contained at the bottom.

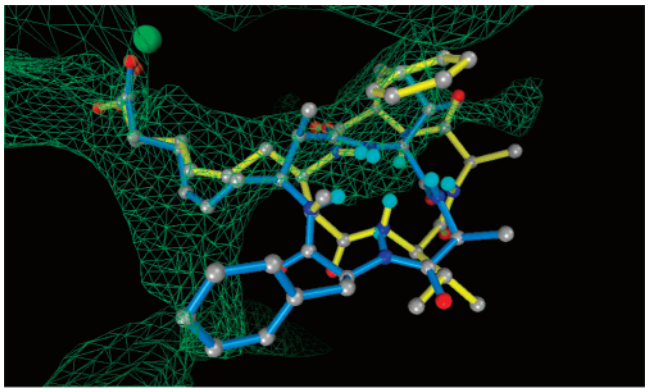

Figure 8. **5** and **8** superimposition in the zinc-binding site. The green mesh represents the hydrophobic pocket of the protein. The Zn^{2+} is represented by a CPK sphere in dark green. **5** is depicted by sticks (yellow) and balls (by atom type: C, gray; polar H, sky blue; N, blue; O, red); **8** is shown by sticks (dark blue) and balls (by atom type: C, gray; polar H, sky blue; N, blue; O, red). The figure highlights the similar interactions with the 11 Å deep hydrophobic channel of the amnda side chains, whereas the phenyl groups of **5** and **8** are located on opposite sides of the receptor surface hydrophobic pocket.

coordinating carboxylate group, forming hydrogen bonds with $H^{\epsilon 2}$ of H131 and H132 and OH of Y297.[35]

The macrolactam accommodates in the shallow pocket delimited by H170, Y196, A197, L265, F198, and F200 amino acids. In this case, the L-Val isopropyl group is placed in a similar position with respect to the L-Phe side chain observed in natural **5** (see Figure 5). Even though such a group does not perfectly interact with the receptor, as observed for the D-Phe side chain of the natural enantiomer, it establishes hydrophobic contacts with Y196, L265, S266, and K267. Further hydrophobic interactions are formed by L-Phe side chain that finds a counterpart delimited by residues P22, Y91, E92, and F141.

The different binding modes of **8** and **5**, with respect to the HDLP active site, are highlighted in Figure 8. From this superimposition, it can be well appreciated the inverse arrangement of the peptide bonds and the resemblant positioning of the enantiomers' cap groups.

The different arrangement of the (−)-azumamide E (**8**) and the suboptimal hydrophobic interactions are responsible for a predicted decrease in the binding affinity to the receptor of about 40-fold (K_i of azumamide E 3.5×10^{-9} vs K_i of the enantiomer 1.4×10^{-8}). Such a decrease is in a good qualitative accordance

Table 1. Biological Activities of **5**, **7**, and **8** on HeLa NE

compound	**5**	**7**	**8**
IC_{50} (μM)[a]	0.134 (±0.024)	N.A. at 50 μM	26.0 (±4.4)

[a] Values are means of at least two independent experiments.

to the results of biological essays (IC_{50} values of 0.134 μM and 26 μM, respectively; see Table 1).

Biological Activities. (+)-Azumamide E (**5**), (2*R*,3*S*)-azumamide E (**7**), and (−)-azumamide E (**8**) showed distinct effects on the HDAC enzymatic activity associated with nuclear extracts (NE) prepared from HeLa cells (Table 1).

As predicted by the docking studies, the (2*R*,3*S*)-azumamide E (**7**) showed no measurable inhibitory activity in this assay up to a concentration of 50 μM. In contrast, both (+)-azumamide E (**5**) and (−)-azumamide E (**8**) displayed inhibitory activities, albeit the enantiomer showed a significant loss in potency, thus confirming that the side chain topology is an important determinant for the biological activity of these cyclotetrapeptides. Extensive profiling of (+)-azumamide E (**5**) revealed that this compound is an isoform-selective HDAC inhibitor, displaying potent inhibition of HDAC 1−3, weaker activity on HDAC8, and more severe decrease in potency on HDAC 4−7, 9 (Table 2).

Table 2. Biological Activities of **5** on HDAC Isoforms

HDAC subtype	1	2	3	4	5	6	7	8	9
IC_{50} (μM)[a]	0.050 (±0.001)	0.100 (±0.033)	0.080 (±0.007)	30% at 50 μM	10.0 (±0.7)	12.0 (±2.7)	9.7 (±1.2)	3.7 (±0.7)	28.0 (±4.9)

[a] Values are means of at least two independent experiments.

In summary, **5** is a potent, selective inhibitor of class I HDACs 1−3. The inhibitory activity on these recombinant enzymes is similar to that measured on HeLa NE. This is consistent with the observation that endogenous HDAC 1, 2, and 3 account for most of the enzymatic activity associated with NE (unpublished results). While it is documented that HDAC 6 (class IIb) is relatively resistant to the inhibition by cyclopeptide compounds,[19b] the significant loss of potency shown by class IIa HDACs (4, 5, 7, and 9) is, to our knowledge, unprecedented.[36]

Conclusion

Cyclic peptides constitute the most structurally complex and diverse class of HDAC inhibitors. Our combined efforts clarify the action of the most powerful natural carboxylic acid containing HDAC-inhibitor known to date[37] and unravel, at molecular level, the high HDLP binding affinity conferred by the unique azumamides cyclotetrapeptide scaffold cap group.

Accumulating data suggests that each subtype of the HDAC family plays a different role in the gene expression,[38] and cyclic tetrapeptides scaffold, with their ample set of surface contacts, can, in principle, target enzyme specificity through proper modulation of the amino acid configurational and structural assortment. Our integrated studies demonstrate the relevance of the side chain topology and the limited impact of the peptide bond orientation in terms of binding affinity and HDAC inhibitory activity. In particular, in a rational design of new peptidomimetic HDAC inhibitors, novel targets should be selected among those presenting proper appendages morphology.

In conclusion, we have designed and stereoselectively synthesized appropriate topochemical variants of natural (+)-azumamide E (**5**). Accurate docking studies and concurrent biological testing allowed us to derive a plausible model for the interaction of azumamides with the HDLP binding pocket and to highlight the critical features necessary for the optimal contact modes.

Acknowledgment. Financial support from the MIUR ("Sintesi di Sostanze Naturali e di loro analoghi sintetici con attività antitumorale") and the Università degli Studi di Salerno. Both the institutions are gratefully acknowledged. We also thank Dr. Patrizia Iannece for mass spectra and Miss Chiara De Cola for experimental work.

Supporting Information Available: Experimental procedures for all new compounds (**7**, **8**, **10**−**24**); ^{1}H and ^{13}C NMR, HSQC for **7** and **8**; 2D-ROESY for **5** and **7**; table of the ROESY cross-peak volumes; list of significant distances in the 3D docking model between **5**, **7**, and **8** and the HDLP binding site; values of inhibition constants and energies associated with the calculated complex; ChelpG calculated charges for **5**, **7**, and **8**. This material is available free of charge via the Internet at http://pubs.acs.org.

JA0686256

(36) For non-cyclopeptide compounds showing selective class I HDAC inhibitory activity, see: Jones, P.; Altamura, S.; Chakravarty, P. K.; Cecchetti, O.; De Francesco, R.; Gallinari, P.; Ingenito, R.; Meinke, P. T.; Petrocchi, A.; Rowley, M.; Scarpelli, R.; Serafini, S.; Steinkühler, C. *Bioorg. Med. Chem. Lett.* **2006**, *16*, 5948−5952.

(37) The most powerful, carboxylic acid containing inhibitor known is semisynthetic and is reported in ref 19d (IC_{50}: 15 nM, HDAC derived from partially purified extracts of human HeLa cells). Usually, synthetic carboxylic acid containing inhibitors show activity in μM range. The only exception (IC_{50}: 200 ± 100 nM) can be found in Woo, S. H.; Frechette, S.; Khalil, E. A.; Bouchain, G.; Vaisburg, A.; Bernstein, N.; Moradei, O.; Leit, S.; Allan, M.; Fournel, M.; Trachy-Bourget, M.-C.; Li, Z.; Besterman, J. M.; Delorme, D. *J. Med. Chem.* **2002**, *45*, 2877−2885.

(38) (a) Brehm, A.; Miska, E. A.; McCance, D. J.; Reid, J. L.; Bannister, A. J.; Kouzarides, T. *Nature* **1998**, *391*, 597−601. (b) Magnaghi, J. L.; Groisman, R.; Naguibneva, I.; Robin, P.; Lorain, S.; Le, Villain. J. P.; Troalen, F.; Trouche, D.; Harel-Bellan. A. *Nature* **1998**, *391*, 601−605. (c) Lemercier, C.; Verdel, A.; Galloo, B.; Curtet, S.; Brocard, M. P.; Khochbin, S. *J. Biol. Chem.* **2000**, *275*, 15594−15599.